Invited paper

Palas Roy* and Jyotishman Dasgupta

Temporal probing of excitons in organic semiconductors

Abstract: Photoinduced charge generation forms the physical basis for energy conversion in organic photovoltaic (OPV) technology. The fundamental initial steps involved are absorption of light by organic semiconductors (generally π-conjugated polymers) to generate photoexcited states (Frenkel excitons) followed by charge transfer and charge separation processes in presence of suitable acceptor. The absorbed photon energy must be utilized completely for achieving maximum device efficiency. However progressive relaxation losses of instantaneously generated high-energy or hot-excited states form major bottleneck for maximum derivable voltage. This efficiency limiting factor has been challenged recently by the role of hot-carriers in efficient generation of charges. Therefore tailoring the dissociation of hot-exciton to be temporally faster than all relaxation processes could minimize the energy loss pathways. Implementation of this concept of hot-carrier photovoltaics demands critical understanding of molecular parameters that circumvent all energy relaxation processes and favor hot-carrier generation. In my dissertation work, I have examined the fate of photo-generated excitons in the context of polymer backbone and morphology, and therefore obtain a fundamental structure-function correlation in organic semiconductors.

Keywords: 2018 IUPAC-Solvay Award; conjugated polymer; exciton; IUPAC-SOLVAY International Award for Young Chemists; organic semiconductors; photovoltaics; polaron pair; polaron; transient absorption.

Introduction

Solar energy is perceived to be a potent renewable energy source for circumventing the present energy crunch arising due to rapid depletion of our fossil fuel reserves [1, 2]. A big surge for harvesting solar light had led to the development of silicon photovoltaics technology with impressive power conversion efficiency (PCE ~24 %). However high fabrication cost for crystalline silicon limits its marketability [3, 4]. Design and development of conjugated polymers which show semiconductor-like properties [5] have opened new avenue towards utilizing these remarkable class of materials for fabricating organic solar cells due to their low-cost processibility, mechanical flexibility and chemically tunable optoelectronic properties. Despite their promise in photovoltaic applications, organic semiconductors are limited by moderate power conversion efficiencies due to poor interfacing with electrodes, narrow absorption coverage of the solar radiation, moderate charge mobilities, and large electron-hole (exciton) binding energies [6, 7]. An elegant way to deal with large binding energies and slow charge carrier mobilities is to create charge transfer (or donor-acceptor) interfaces in presence of a suitable acceptor within the active layer of the solar cell which allows for easier separation of charges. Therefore in order to enhance the efficiency of solar cell, guidelines for rational modifications in the

*Corresponding author: Palas Roy, Department of Chemical Sciences, Tata Institute of Fundamental Research, Mumbai-400005, India; and School of Chemistry, University of East Anglia, Norwich NR4 7TJ, UK, e-mail: palas.1989@gmail.com

Jyotishman Dasgupta: Department of Chemical Sciences, Tata Institute of Fundamental Research, Mumbai-400005, India

molecular materials and device engineering is required. These guidelines can only be formulated by directly probing the fate of the instantaneously generated exciton and its dissociation into charges.

Active layer of organic solar cells typically comprise of interpenetrating nano-domains of pure donor polymer and acceptor fullerene phases, also known as bulk heterojunctions (BHJs) as shown in Fig. 1. Absorption of light by the conjugated polymer leads to generation of Frenkel exciton that hops to the donor:acceptor interface followed by generating charge transfer exciton [8]. This interfacial CT exciton undergoes dissociation giving rise to polaron (charges bound by the lattice distortion) and free charges [8]. The corresponding potential energy diagram has been presented in Fig. 2. Efficient conversion of light to electricity in a solar cell faces many obstacles. The theoretically maximum efficiency of an ideal single junction solar cell (under one sun illumination) is limited to 33 %, also known as Shockley–Queisser limit [9]. The four primary consideration in this calculation are: (i) losses caused by thermalization of charge carriers generated by absorbing high-bandgap energy photons, (ii) losses due to recombination of the charge carriers, (iii) losses due to inability to absorb photons with low-bandgap energy and (iv) low absorption efficiency of a device. In fact high-bandgap energy photons only excite one electron per photon which ultimately ends up at the bottom of the conduction band. In order to exceed this intrinsic efficiency limit, it is important to understand the fundamental loss mechanisms. The photon-to-charge conversion efficiency (η) of solar cell is proportional to the short-circuit current (I_{sc}) and open-circuit voltage (V_{oc}) of the device which are in turn dictated by these photoinduced processes in the device. The total number of charges collected at the electrode determines the I_{sc} of device. However competitive processes such as geminate and nongeminate recombination always hinder the separation of charges and reduce I_{sc} of the system. In principle, higher I_{sc} can be obtained by reducing the bandgap of polymers so as to harvest more solar light from longer wavelengths. In fact, much effort has been made in generating multiexcitonic states per photon absorbed. Recently, singlet fission has perceived a vital importance as it has the potential to achieve photo-conversion efficiency beyond Shockley-Queisser limit of 33 % [10].
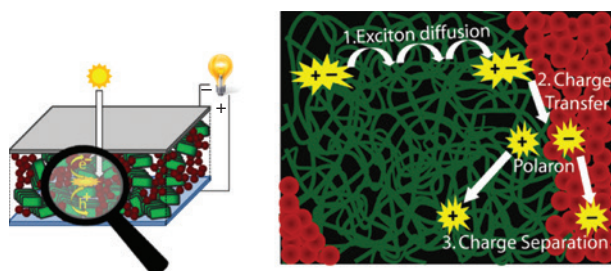

Fig. 1: Illustration of photoinduced processes in the active layer of BHJ solar cells: exciton generation, exciton diffusion to the polymer:fullerene interface, charge transfer leading to generation of polaron pair and charge separation. Green lines and red balls represent polymer and fullerene phases respectively.
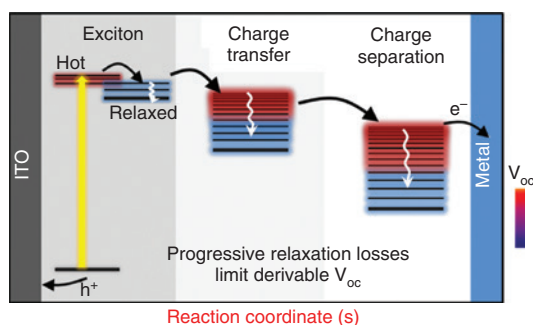

Fig. 2: Potential energy diagram depicting photoinduced processes: exciton generation, charge transfer and charge separation. Progressive relaxation loss limits the maximum V_{oc} of device and the total charges collected at the electrode determine I_{sc}.

On the other hand, V_{oc} of a device is limited by the energy difference between HOMO of the donor and LUMO of the acceptor [11]. Typically V_{oc} of an organic solar cell is much lower compared to the energy of the photons absorbed. This forms major drawback for organic photovoltaic devices. There are several loss mechanisms contributing to loss of V_{oc}, such as (a) fast internal conversion in the singlet exciton manifold, (b) relaxation to the lower energy charge transfer states, and (c) energy offset at molecule-electrode interface. Solar cell with high V_{oc} has been realised recently using non-fullerene based acceptors because of minimal energy loss during exciton to charge transfer state transition. As a result, tuning the bandgap of the active layer materials without sacrificing efficient charge generation as well as high V_{oc} becomes a major hurdle in achieving high-efficiency organic solar cell.

The efficiency of photo-induced charge generation at BHJ interfaces is critically dictated by the bandgap of the electron donor polymer as well as the absolute energies of the donor HOMO and the acceptor LUMO levels [11]. Although large band gap (~2.2 eV) homo-polymers like poly(3-hexylthiophene) (P3HT) have been champion material for long time, they cannot harvest near infrared (NIR) photons of the solar spectrum. This leads to the development of novel low bandgap polymers (1.6–1.8 eV) with alternating arrangement of electron donating and accepting moieties along the conjugated backbone. Recently, such donor-acceptor co-polymers with fullerenes form efficient organic solar cells with record breaking power conversion efficiencies (PCE) of ~11 % [12]. In order achieve the Shockley–Queisser limit of 33 % [10], it is imperative to understand all the non-radiative energy loss pathways subsequent to the generation of exciton in such complex polymer backbone. Based on several reports, the instantly generated hot delocalized exciton on pristine homo-polymer backbone can undergo different relaxation pathways as picturized in Fig. 3: exciton self-trapping (<30–100 fs), local torsional relaxation (~200–500 fs) and excitonic energy transfer (~1–10 ps) processes [13]. On the other hand, donor-acceptor type polymer framework having additional complexity of inter-chromophore torsions and added degrees of freedom can provide multiple and sometimes complex relaxation pathways in the excited state. This results into loss of photon energy thereby reducing the open circuit voltage (V_{oc}) of the device. In fact, photo-excitation of low-bandgap polymer can lead to instantaneous generation of polaron pair apart from exciton formation. In order to optimize the charge generation yields with respect to exciton relaxation pathways, it is imperative to track the fate of instantaneously generated excitons in the organic backbone using high temporal precision. Such an effort will identify the important molecular coordinate(s) that drive variety of photoinduced processes such as exciton relaxation and provide guideline for making future efficient materials.

Formation of complex microstructure upon film casting is one of the remarkable features of organic semiconductors. The numerous degrees of conformational freedom of the polymer backbone dictate its crystallinity in films via modulation of intermolecular packing. The crystalline domains of the solvent-casted polymer films are believed to have exciton that can get more delocalized leading to its efficient dissociation to charges via ultrafast exciton diffusion to the *polymer:fullerene* interface [14]. The subtle interplay between excitons and charges in different domains of the polymer film can alter the charge carrier yields, and thus the overall I_{sc} of the device. Nanoscopic structure of the domains has been observed to strongly affect the efficiency of the exciton diffusion and its dissociation [15–19]. Since the morphology of the films is critically dependent on the nature of the polymer and its solvent processing conditions [20], comprehensive understanding of the film casting process is significant for optimizing device efficiency.
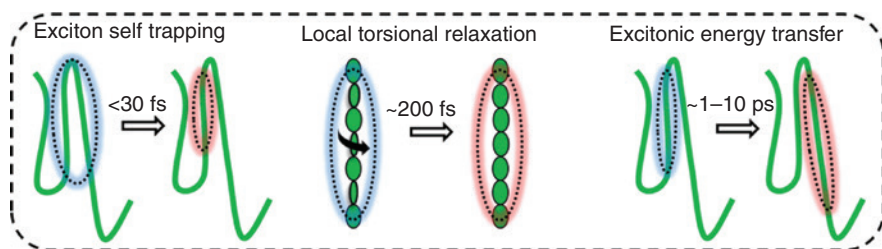

Fig. 3: Schematic representation of different types of exciton relaxation processes in conjugated polymers.

My PhD thesis work aims to experimentally track the fate of photogenerated excitons and probe the reaction coordinates leading to exciton relaxation, charge transfer, and ultrafast triplet formation in organic semiconductors. I examine these results in the context of polymer backbone and its morphology. Our work provides a detailed understanding of the fundamental structure-function correlation for organic semiconductors. Main contribution of my thesis belongs to: (1) describing the role of bridge moiety in an electron donor-bridge-acceptor based low-bandgap conjugated polymers in driving exciton relaxation; (2) emphasizing the role of film crystallinity on exciton dissociation; (3) exploring the role of solvent in dictating the morphology of polymer:fullerene interfaces in films; and (4) describing the role of molecular packing in determining ultrafast triplet generation rates.

Results and discussion

Contribution 1. Exciton relaxation and polaron pair generation in copolymer

Donor-π-acceptor copolymers form the material basis for achieving record efficiencies in modern OPVs. It is conjectured that large dipole moment change upon photoexcitation via intramolecular charge transfer (ICT) in donor-π-acceptor backbone facilitates efficient charge-carrier generation [21, 22]. However, the primary structural changes that drive ultrafast ICT are difficult to comprehend using time-resolved electronic spectroscopy due to convoluted spectra of multiple intervening excited states. We built structure-sensitive femtosecond stimulated Raman spectroscometer (FSRS) in our lab at TIFR, Mumbai and demonstrate that π-bridge torsion forms the primary reaction coordinate for ICT in poly(thiophene-diketopyrrolopyrrole-benzobithiophene) (TDPP-BBT), having an intrinsic thiophene bridge that couples the individual BBT donor and DPP acceptor moieties. Resonance Raman snapshots of exciton relaxation reveal rich vibrational dynamics of the bridge modes associated with ~400 fs backbone planarization leading to hot-ICT state formation while cooling dynamics of backbone-centric modes probe the ICT relaxation in 1–10 ps (Fig. 4) [23]. Therefore synthetically tuning the thiophene bridge torsion timescale in donor-π-acceptor copolymer by introducing non-covalent interaction between bridge and other structural parts of polymer will ensure hot-CT generation while minimizing relaxation processes. This establishes a phenomenological gating role of bridge torsions in
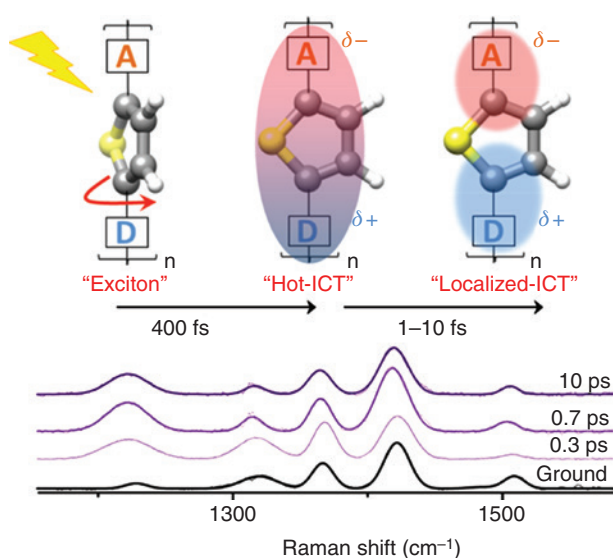

Fig. 4: Ultrafast thiophene bridge planarization in donor-bridge-acceptor copolymers tracked using femtosecond stimulated Raman spectroscopy.

determining the fundamental timescale and energy of photo-generated carriers and opens up new synthetic guidelines for fabricating energy-efficient OPVs.

Contribution 2. Effect of alkyl side chains on polaron generation in P3HT films

Designing π-conjugated backbones with side-chains primarily utilized as solubilizing groups is the most critical step to tune film morphology in OPVs [24–27]. Here we used transient absorption spectroscopy to report the formation dynamics of charge-carriers in a well celebrated conjugated polythiophene backbone with different branching of side-chains: linear hexyl group (in P3HT) versus branched 2-ethylhexyl group (in P3EHT). Photoexcitation of P3HT films generate charge carriers like exciton, polaron and polaron pair whose absorption spectra are well assigned [28] and their corresponding absorption bands come at around 1200 nm, 1000 nm and 650 nm respectively. Spectral comparison in Fig. 5 shows that exciton and polaron bands are red shifted in P3HT film compared to P3EHT film. This indicates that higher crystallinity of P3HT films result into delocalized excitons and polarons compared to that in P3EHT. In fact, weakly bound polaron pairs are observed only in P3HT film thereby highlighting the importance of crystalline morphology. Therefore crystallinity of polymer film and delocalized nature of photoexcitations play a gating role for hot-carrier generation. If these charge-carriers are to be harvested in OPV devices, the charge extraction at electrode interface needs to be carried out within the lifetime of polaron (455 ps) and polaron pair (42 ps) that provide insight into the length scale of thin polymer films. Our work motivates new experimental studies on different types of single molecular junctions [29] that can provide enormous information on tuning the interface.

Contribution 3. Charge generation in the soluble P3HT:PCBM nanoaggregates

The film processing conditions also play critical role for tuning its morphology [30–33]. The interpenetrated nano-domains of polymer and fullerene form the basis of active layer morphology in bulk-heterojunction solar cell. The effect of solvent on dried film morphology brings the hypothesis of preformed solution structure. Janssen and coworkers used thermodynamic framework to propose a polymer:fullerene:solvent ternary phase that exist between solution and dried film phases [34]. In fact Lee et al performed coarse-grain MD simulation to show that different solution structures exist in different solvents [35]. Synthetic control on blend morphology can only emanate from detailed understanding of intermediate polymer:fullerene solution structures during film casting process. Here we use photoinduced charge generation rates to probe the effective domain
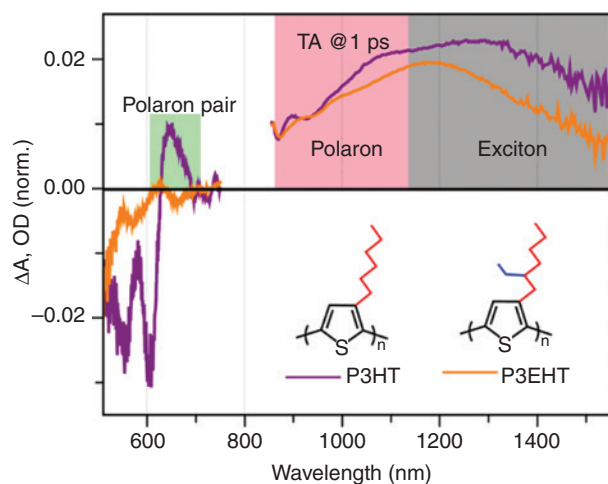

Fig. 5: Femtosecond transient absorption spectra of polythiophene with different side chains.
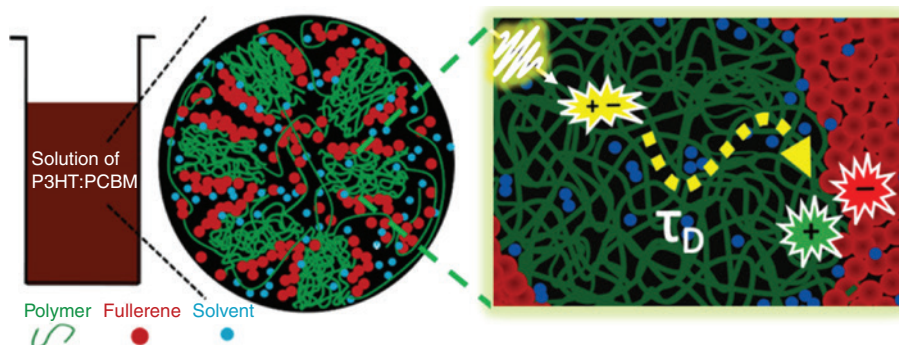
Fig. 6: Schematic representation of exciton dissociation to generate charges in soluble polymer:fullerene nano-aggregates.

size of pre-formed solution structures arising from a mixture of poly(3-hexylthiophene-2,5-diyl) (P3HT) and [6, 6]-phenyl-C61-butyric acid methyl ester (PCBM) in three different organic solvents. Using femtosecond transient absorption spectroscopy, we observed solvent dependent biphasic rise of polaron signatures within the soluble P3HT:PCBM nano-aggregates (Fig. 6) analogous to that observed in annealed films [36–38]. Using the diffusive component of charge generation, we find P3HT:PCBM mixtures in toluene exhibit ~3 times larger functional domain sizes than chlorobenzene thereby correctly predicting the eventual film morphology [39]. We thus provide first experimental evidence for the postulated polymer:fullerene:solvent ternary phase that seeds the eventual dried film morphology. Our work motivates design of new chemical additives to tune grain size of the evolving polymer:fullerene nano-domains in solution for fabricating hot-carrier OPVs.

Contribution 4. Ultrafast singlet fission in diketopyrrolopyrrole nanoparticles

Other than optimizing active layer and organic-metal interface, incorporation of singlet exciton fission (SF) layer in a photovoltaic device has recently received broad attention as it can generate two excited state populations by absorbing only one photon (Fig. 7) [40]. For SF to occur, the energy of chromophore should follow E(S1) ≥2*E(T) and they should be electronically coupled well. One of the intriguing class of chromophores is diketopyrrolopyrrole (DPP), which has high molar cross-section, robust than other SF materials, a p-type semiconductor and follows the energy criteria for SF [41, 42]. Femtosecond transient absorption spectroscopy in aqueous suspension of DPP nanoparticle tracks the rise of excited state absorption around 610 nm (Fig. 7) which is known to be triplet signature in DPP molecules as is also shown by Wasielewski and coworkers [43]. The formation of correlated triplet pair (T-T) intermediate within 700 fs concomitant with decay of singlet exciton is unequivocal evidence for ultrafast SF in DPP nanoparticles. Based on global analysis, nanosecond flash photolysis and time-resolved emission measurements, we show that the T-T pair population dissociates in 9 ps to form free triplets with 130 % quantum efficiency while rest of it recombines to regenerate singlet states. Therefore optimal packing of DPP molecules within crystalline nano-aggregates ensures efficient SF thereby introducing new material morphology. We envision that by optimizing nanoparticle morphology of such DPP aggregates, SF layer can be effectively used for charge injection in OPVs.

Future prospectives

My PhD dissertation provides comprehensive information about the photophysics of organic semiconductors via tailoring their chemical structure and film morphology. Our work highlights the plausible future directions that can enrich our understanding on structure-function correlation in OPVs.
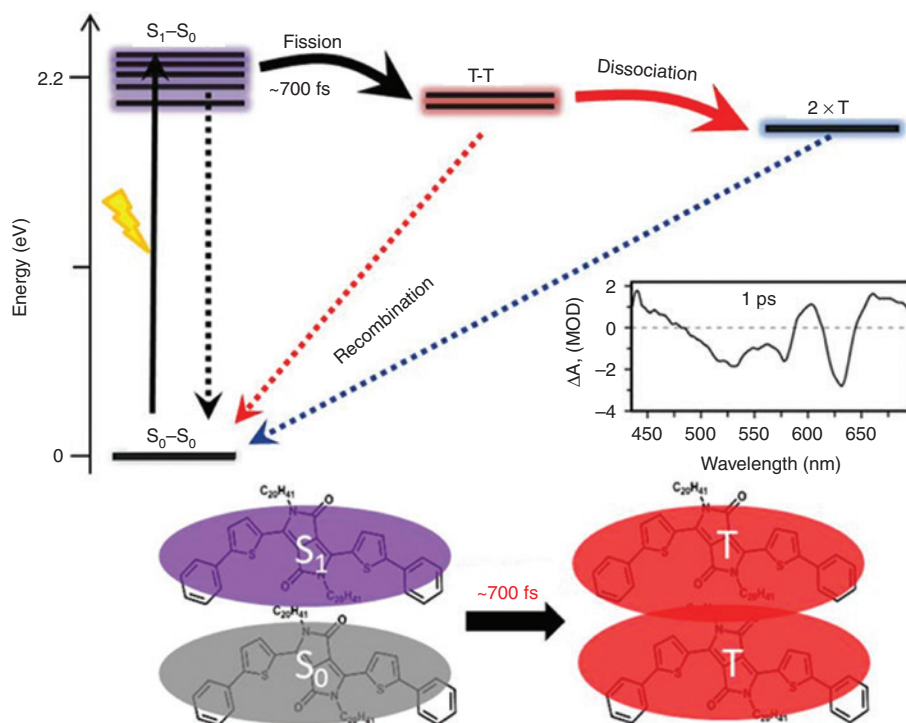
Fig. 7: Energy level diagram and femtosecond transient absorption spectra of DPP nanoparticles showing singlet fission.

1. Choice of organic semiconductors and processing film morphology: In order to implement the concept of hot-carrier photovoltaics, critical understandings of the molecular parameters that circumvent all the energy relaxation processes and favor hot-carrier generation are required. My dissertation work proposed that synthetically tuning the thiophene bridge torsion timescale in donor-bridge-acceptor copolymer by introducing non-covalent interaction between the bridge and other chemical entity of the polymer will help to slow down relaxation processes while ensuring hot CT generation. In addition, my dissertation work highlights that the generation of delocalized photoexcitations that plays a gating role for hot-carrier generation can be favored by tuning crystallinity of polymer film tuned by sidechain engineering or by designing new solvent additives. Our work provides new design principles for fabricating hot-carrier organic photovoltaics by tuning both material property and film morphology. In future, resonance selective FSRS measurements along with multi-dimensional impulsive Raman experiments in order to decipher the mode couplings [44–46] will provide a unified picture on hot-carrier generation on variety of organic semiconductors. In addition, Femtosecond optical Kerr effect spectroscopy [47] can be implemented to exhibit long-range global modes involved in hot-carrier generation. On the other hand, time-resolved optical and electron microscopy [48–50] can also selectively interrogate and image photoexcitations moving within a working device. Our findings will inspire new computational efforts to understand the nature of the vibronic coupling that drives the generation of observable transient hot-states.

2. Interfacing the organics with metal electrodes: Even after efficient dissociation of charge carriers at the active layer, they encounter each other at the organic-electrode interface and recombine back to the ground state leading to a major loss in device performance. Therefore, it is imperative to collect the charges immediately at the organic-metal interface before they undergo recombination. My dissertation work has provided information on polaronic state in conjugated polymers that are short-lived (lifetime ~40 ps). In order to harvest such polarons in a photovoltaic device, the charge extraction at the organic-electrode interface needs to be carried out within this short time window. This provides insight into using thin polymer films at the electrode interface that can extract charges directly without added acceptors. In future, it will be important to understand the charge injection and recombination processes at the interface between conjugated

polymer and metal electrodes in a device. Our work inspires new experimental studies on different types of single molecular junctions [51] (i.e. molecule-electrode interface) that can provide enormous information on tuning the interface.

3. Exploring novel ways for multiple exciton generation: Other than optimizing active layer and the organic-metal interface, ways to generate multiexciton have shown great promises to enhance device performance beyond the Shockley–Queisser limit [10]. My dissertation work on singlet exciton fission in DPP-nanoparticles will inspire new experiments to understand the ultrafast generation of transient T-T state. In future, resonance selective FSRS measurements along with Impulsive Raman spectroscopy [52] and multidimensional electronic spectroscopy [53] can provide enormous information about the reaction trajectory for ultrafast singlet exciton to triplet conversion. We envision that by optimizing the morphology of such DPP nanoaggregates via sidechain engineering or changing the processing condition, the SF layer can be effectively used for charge injection in next generation OPVs with high device efficiency.

Conclusion

In my PhD thesis work, I have probed the molecular basis for choosing the photo-active layer and its morphology to achieve control on the fate of excitons in organic semiconductors for photovoltaic applications. Our focus has been to temporally track the evolution of the excitons in both solution and films of conjugated polymers using time-resolved absorption and vibrational spectroscopy. Understanding charge transfer process is central to designing efficient organic photovoltaics, but it remains challenging to track the molecular coordinate(s) that drive charge transfer. Using structure-sensitive femtosecond stimulated Raman spectroscopy, we monitor real-time structural changes in donor-π-acceptor copolymer backbone, and enumerate the role of π-bridge torsions during intramolecular charge transfer. We propose that synthetically tuning the thiophene bridge torsion timescale in donor-π-acceptor copolymer will help to slow down relaxation processes while ensuring hot CT generation.

We have also put in an effort to understand the relevance of film morphology in dictating exciton lifetime and charge generation yields. In order to tune crystallinity of spin-casted polymer film, we used chemically distinct side-chains on a common polythiophene backbone. We found the crystallinity of polymer film can be correlated with the generation of delocalized photoexcitations and hot-carriers. Additionally, we identified that the critical step of morphology control occurs directly in the solution of polymer:fullerene itself. Using time-resolved methods to measure charge transfer within solution aggregates of polymer:fullerenes, we provided the first experimental evidence for polymer:fullerene:solvent ternary phase that seeds the eventual film morphology. Therefore optimizing the solvent controlled ternary interactions in solution itself is crucial for designing the morphology of the active film in bulk heterojunction solar cells. These findings open up new guidelines for increasing hot-carriers in organic photovoltaics by tuning both material property and film morphology. Morphological controls on the packing of organic semiconductors also allow for the discovery of new photophysical processes, like singlet fission (SF). We demonstrate unequivocally that packing diketopyrrolopyrrole chromophores within crystalline nanoaggregates ensures high efficiency SF process using femtosecond broadband transient absorption spectroscopy in conjunction with time-resolved emission measurements. Our work should inspire new computational and experimental efforts in understanding the nature of the vibronic coupling that drives the generation of observable transient T-T state.

References

[1]   *Renewable Energy Policy Network for the 21st Century. 2009. Renewables global status report 2009* (2009).

[2]   *Energy Information Administration. 2009. International Energy Outlook 2009. Report # DOE/EIA-0484* (2009).

[3]   A. Wang, J. Zhao, M. A. Green. *Appl. Phys. Lett.* **57**, 602 (1990).

[4]   A. F. B. Braga, S. P. Moreira, P. R. Zampieri, J. M. G. Bacchin, P. R. Mei. *Sol. Energy Mater. Sol. Cells* **92**, 418 (2008).

[5]   A. J. Heeger, A. G. MacDiarmid, H. Shirakawa. *The Royal Swedish Academy of Sciences* (2000).

[6]   R. A. J. Janssen, J. Nelson. *Adv. Mater.* **25**, 1847 (2012).

[7]   D. Wöhrle, D. Meissner. *Adv. Mater.* **3**, 129 (1991).

[8]   M. A. Stevens, C. Silva, D. M. Russell, R. H. Friend. *Phys. Rev. B* **63**, 165213 (2001).

[9]   W. Shockley, H. J. Queisser. *J. Appl. Phys.* **32**, 510 (1961)

[10] V. A. Trukhanov, V. V. Bruevich, D. Y. Paraschuk. *Sci. Rep.* **5**, 1 (2015).

[11] B. Kippelen, J.-L. Bredas. *Energy Environ. Sci.* **2**, 251 (2009).

[12] S. Zhang, L. Ye, J. Hou. *Adv. Energy Mater.* **6**, 1502529 (2016).

[13] C. Consani, F. Koch, F. Panzer, T. Unger, A. Köhler, T. Brixner. *J. Chem. Phys.* **142**, 212429 (2015).

[14] J. Mei, Z. Bao. *Chem. Mater.* **26**, 604 (2013).

[15] A. L. Ayzner, S. C. Doan, B. T. de Villers, B. J. Schwartz. *J. Phys. Chem. Lett.* **3**, 2281 (2012).

[16] H. M. Heitzer, B. M. Savoie, T. J. Marks, M. A. Ratner. *Angew. Chem. Int. Ed.* **53**, 7456 (2014).

[17] R. J. Kline, M. D. McGehee, E. N. Kadnikova, J. Liu, J. M. J. Fréchet. *Adv. Mater.* **15**, 1519 (2003).

[18] R. Noriega, J. Rivnay, K. Vandewal, F. P. V. Koch, N. Stingelin, P. Smith, M. F. Toney, A. Salleo. *Nat. Mater.* **12**, 1038 (2013).

[19] K. Maturová, S. S. V. Bavel, M. M. Wienk, R. A. J. Janssen, M. Kemerink. *Nano Lett.* **9**, 3032 (2009).

[20] J. J. van Franeker, G. H. L. Heintges, C. Schaefer, G. Portale, W. Li, M. M. Wienk, P. van der Schoot, R. A. J. Janssen. *J. Am. Chem. Soc.* **137**, 11783 (2015).

[21] R. Tautz, E. D. Como, T. Limmer, J. Feldmann, H.-J. Egelhaaf, E. von Hauff, V. Lemaur, D. Beljonne, S. Yilmaz, I. Dumsch, S. Allard, U. Scherf. *Nat. Commun.* **3**, 970 (2012).

[22] B. S. Rolczynski, J. M. Szarko, H. J. Son, Y. Liang, L. Yu, L. X. Chen. *J. Am. Chem. Soc.* **134**, 4142 (2012).

[23] P. Roy, A. Jha, V. B. Yasarapudi, T. Ram, B. Puttaraju, S. Patil, J. Dasgupta. *Nat. Commun.* **8**, 1716 (2017).

[24] E. F. Manley, T. Harschneck, N. D. Eastham, M. J. Leonardi, N. Zhou, J. Strzalka, R. P. H. Chang, L. X. Chen, T. J. Marks. *Chem. Mater.* **31**, 8308 (2019).

[25] Z. Guo, D. Lee, R. D. Schaller, X. Zuo, B. Lee, T. Luo, H. Gao, L. Huang. *J. Am. Chem. Soc.* **136**, 10024 (2014).

[26] N. E. Jackson, B. M. Savoie, T. J. Marks, L. X. Chen, M. A. Ratner. *J. Phys. Chem. Lett.* **6**, 77 (2015).

[27] J. Mei, Z. Bao. *Chem. Mater.* **26**, 604 (2014).

[28] O. J. Korovyanko, R. Osterbacka, X. M. Jiang, Z. V. Vardeny. *Phys. Rev. B* **64**, 235122 (2001).

[29] W. Chen, J. R. Widawsky, H. Vázquez, S. T. Schneebeli, M. S. Hybertsen, R. Breslow, L. Venkataraman. *J. Am. Chem. Soc.* **133**, 17160 (2011).

[30] Y. Kim, S. Cook, S. M. Tuladhar, S. A. Choulis, J. Nelson, J. R. Durrant, D. D. C. Bradley, M. Giles, I. McCulloch, C. S. Ha, M. Ree. *Nat. Mater.* **5**, 197 (2006).

[31] Z. Bi, H. Bilal, N. Y. Mao, H. Yan, W. Ma. *Macromolecules.* **51**, 6682 (2018).

[32] B. Walker, A. Tamayo, D. T. Duong, X.-D. Dang, C. Kim, J. Granstrom, T.-Q. Nguyen. *Adv. Energy Mater.* **1**, 221 (2011).

[33] Y. Yao, J. Hou, Z. Xu, G. Li, Y. Yang. *Adv. Funct. Mater.* **18**, 1783 (2008).

[34] S. Kouijzer, J. J. Michels, M. van den Berg, V. S. Gevaerts, M. Turbiez, M. M. Wienk, R. A. J. Janssen. *J. Am. Chem. Soc.* **135**, 12057 (2013).

[35] C.-K. Lee, C.-W. Pao. *J. Phys. Chem. C* **118**, 11224 (2014).

[36] J. Guo, H. Ohkita, H. Benten, S. Ito. *J. Am. Chem. Soc.* **132**, 6154 (2010).

[37] D. Herrmann, S. Niesar, C. Scharsich, A. Köhler, M. Stutzmann, E. Riedle. *J. Am. Chem. Soc.* **133**, 18220 (2011).

[38] A. A. Paraecattil, N. Banerji. *J. Am. Chem. Soc.* **136**, 1472 (2014).

[39] P. Roy, A. Jha, J. Dasgupta. *Nanoscale.* **8**, 2768 (2016).

[40] M. W. B. Wilson, A. Rao, B. Ehrler, R. H. Friend. *Acc. Chem. Res.* **46**, 1330 (2013).

[41] C. M. Mauck, P. E. Hartnett, E. A. Margulies, L. Ma, C. E. Miller, G. C. Schatz, T. J. Marks, M. R. Wasielewski. *J. Am. Chem. Soc.* **138**, 11749 (2016).

[42] P. E. Hartnett, E. A. Margulies, C. M. Mauck, S. A. Miller, Y. Wu, Y.-L. Wu, T. J. Marks, M. R. Wasielewski. *J. Phys. Chem. B* **120**, 1357 (2016).

[43] C. M. Mauck, P. E. Hartnett, Y.-L. Wu, C. E. Miller, T. J. Marks, M. R. Wasielewski. *Chem. Mater.* **29**, 6810 (2017)

[44] D. R. Dietze, R. A. Mathies. *ChemPhysChem* **17**, 1224 (2016).

[45] S. M. Falke, C. A. Rozzi, D. Brida, M. Maiuri, M. Amato, E. Sommer, A. De Sio, A. Rubio, G. Cerullo, E. Molinari, C. Lienau. *Science* **344**, 1001 (2014).

[46] D. P. Hoffman, R. A. Mathies. *Acc. Chem. Res.* **49**, 616 (2016).

[47] M. G.-Jiménez, G. Ramakrishnan, T. Harwood, A. J. Lapthorn, S. M. Kelly, E. M. Ellis, K. Wynne. *Nat. Commun.* **7** (2016).

[48] Y. Wan, Z. Guo, T. Zhu, S. Yan, J. Johnson, L. Huang. *Nat. Chem.* **7**, 785 (2015).

[49] T. Zhu, Y. Wan, Z. Guo, J. Johnson, L. Huang. *Adv. Mater.* **28**, 7539 (2016).

[50] M. K. L. Man, A. Margiolakis, S. D.-Jones, T. Harada, E. L. Wong, M. B. M. Krishna, J. Madéo, A. Winchester, S. Lei, R. Vajtai, P. M. Ajayan, K. M. Dani. *Nat. Nanotechnol.* **12**, 36 (2017).

[51] W. Chen, J. R. Widawsky, H. Vázquez, S. T. Schneebeli, M. S. Hybertsen, R. Breslow, L. Venkataraman. *J. Am. Chem. Soc.* **133**, 17160 (2011).

[52] A. J. Musser, M. Liebel, C. Schnedermann, T. Wende, T. B. Kehoe, A. Rao, P. Kukura. *Nat. Phys.* **11**, 352 (2015).

[53] A. P. Spencer, W. O. Hutson, E. Harel. *Nat. Commun.* **8**, 14732 (2017).